MECHANICAL PERFORMANCE AND PERMEABILITY BEHAVIOR OF 41.4 MPA PORTLAND COMPOSITE CEMENT CONCRETE UNDER SEAWATER EXPOSURE CONDITIONS

Nuraziz Handika[1], Hafiyya Izzah Aini[1], Jessica Sjah[1], Oktoria Masniari[2], Tri Eddy Susanto[2], Elfiranahla Chandra Dewi[2]
[1]Department of Civil and Environmental Engineering, Faculty of Engineering, Universitas Indonesia
[2]Department of Research & Development, PT Semen Indonesia (Persero) Tbk
E-mail: n.handika@ui.ac.id

Received 3rd September 2025, Accepted 20th October 2025

ABSTRACT

This study examines the effects of seawater salinity on the mechanical and permeability properties of concrete made with Portland Composite Cement (PCC), a sustainable alternative to Ordinary Portland Cement (OPC) with up to 30% lower CO_2 emissions. Concrete specimens were cured in water ponds with salinity levels of <0.1%, 0.2–0.4%, 0.6–0.7%, and 3–3.5% to simulate coastal exposure. Compressive strength, splitting tensile strength, permeability, and Ultrasonic Pulse Velocity (UPV) were tested at 7, 28, 42, 56, and 90 days. Compressive strength generally increased with age, but the target of 41.4 MPa was not consistently reached by 42 days. High salinity exposure reduced tensile strength and produced more brittle fracture patterns, indicating increased cracking potential. Interestingly, permeability decreased in high-salinity samples, possibly due to salt crystallization within pores, though this was not supported by UPV results. The weak correlation between UPV and both strength and permeability suggest microstructural effects not captured by non-destructive testing alone. PCC concrete showed acceptable performance in low-salinity conditions (<1%), making it suitable for mildly aggressive marine environments. These findings support the broader use of PCC in sustainable construction and highlight the need for further microstructural investigation under saline exposure.

Keywords: *Portland Composite Cement (PCC), Seawater Exposure, Concrete Durability, Compressive Strength, Splitting Tensile Strength, Permeability, Salinity Effects, Sustainable Construction, and Ultrasonic Pulse Velocity (UPV)*

INTRODUCTION

Concrete remains the most widely used material in modern construction, favored for its high load-bearing capacity, availability, and versatility. It plays a crucial role in the development of infrastructure such as high-rise buildings, bridges, and dams (IRICEN 2014). However, the long-term durability of concrete is challenged when exposed to aggressive environments, particularly saline or marine conditions. These environments accelerate the degradation of concrete through various physical and chemical processes, including alkali–aggregate reactions, sulfate attacks, and corrosion of embedded reinforcement—most of which are triggered by the ingress of chloride and sulfate ions (Qasim et al. 2020). Sulfate ions can react with cement hydration products, causing expansive reactions that lead to cracking and structural deterioration (Mehta 1983; Neville 2011). As a result, sulfate-induced damage remains a significant concern for infrastructure in coastal and groundwater-influenced areas (Tian and Cohen 2000).

To address this, standards such as SNI 2049:2015 (BSN Badan Standarisasi Nasional 2013) recommend the use of sulfate-resistant cements, namely, Type II and Type V, for structures exposed to moderate or high sulfate concentrations. Although effective, these cement types are less commonly used in small-scale coastal structures like piers, seawalls, and docks, primarily due to their higher cost and limited accessibility. This limitation underscores the need to investigate alternative cement types that balance technical performance with economic and environmental viability.

In parallel, the cement industry faces increasing pressure to reduce greenhouse gas emissions. Cement production is a major contributor to global CO_2 emissions (United Nations Environment Programme and Global Alliance for Buildings and Construction 2024), largely due to the calcination process (conversion of $CaCO_3$ to CaO) and the combustion of fossil fuels required for clinker formation (Feiz et al. 2015; Gibbs, Soyka, and Conneely 2001). Strategies to lower the carbon footprint of cement include the use of alternative fuels, energy-efficient technologies, and supplementary cementitious materials. Portland Composite Cement (PCC) represents one such alternative, incorporating additives such as blast furnace slag, pozzolans, and silicate compounds to partially replace clinker, thereby reducing CO_2 emissions by up to 30% compared to Ordinary Portland Cement (OPC) (Nasional 2022; SIG 2023).

To comprehensively evaluate the performance of PCC concrete in saline environments, this study incorporated a combination of mechanical and durability-related tests. Compressive strength was measured as a fundamental indicator of load-bearing capacity and material development over time. Splitting tensile strength was assessed to examine the concrete's resistance to cracking, which is crucial in chloride-rich environments that promote steel corrosion. Ultrasonic Pulse Velocity (UPV) testing provided a non-destructive means of monitoring internal concrete quality, homogeneity, and the potential presence of microcracks (Ernawan et al. 2023; Handika, Norita, et al. 2021; Handika, Rafky, et al. 2021; Mangasi et al. 2024). Permeability testing, a durability-related test, was used to evaluate the capacity of saline water to penetrate the concrete matrix, which directly affects the risk of durability loss and reinforcement deterioration. These complementary tests offer a comprehensive understanding of how PCC concrete performs under different levels of salinity exposure.

This study explores the performance of concrete made with PCC when exposed to varying levels of salinity, focusing on both mechanical and durability-related properties. The experimental program involved conventional concrete designed to achieve a target compressive strength of 41.4 MPa, in accordance with SNI 03-6468-2023 (Nasional 2023b). Concrete specimens were cured in water ponds with salinity concentrations of <0.1%, 0.2–0.4%, 0.6–0.7%, and 3–3.5%. Compressive and splitting tensile strengths were evaluated using cylindrical specimens following ASTM standards (ASTM International 2017b, 2021), while cube specimens were tested for permeability based on DIN guidelines (ANSI 1991). By analyzing the influence of salinity and curing duration on PCC concrete, this study provides insights into its suitability for sustainable construction in saline environments, especially where conventional sulfate-resistant cements are economically unfeasible.

METHODS

Materials and Mixing Proportions

This study employed an environmentally friendly Portland Composite Cement (PCC), commercially available in Indonesia and known for its reduced carbon footprint compared to Ordinary Portland Cement (OPC). The mixing water was obtained from a local well at the casting site; however, no detailed characterization (e.g., pH, sulfate content) of the water was performed.

The fine aggregate used was natural Tayan sand sourced from West Kalimantan, while the coarse aggregate consisted of crushed stone. Both aggregates were tested for their physical properties in accordance with ASTM standards. Table 1 summarizes the key aggregate properties, including specific gravity, water absorption, and fineness modulus. Sieve analysis results for both fine and coarse aggregates are presented in Figure 1, along with the upper and lower grading limits as specified in ASTM C33/C33M (American Society of Testing Material ASTM International 2008).

The concrete mix design was prepared following ACI guidelines for conventional concrete. The mix was designed to achieve a target compressive strength of 41.4 MPa, with a water-to-cement (w/c) ratio of 0.28. The final mix proportions are detailed in Table 2.

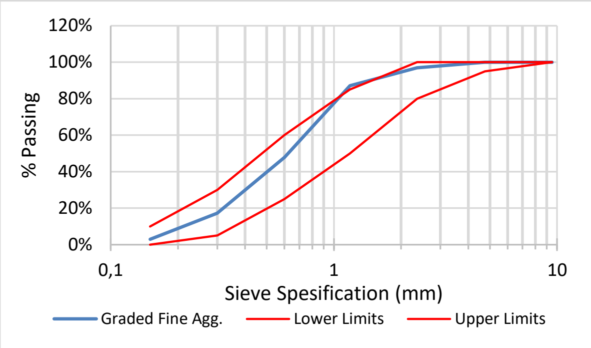

(a)

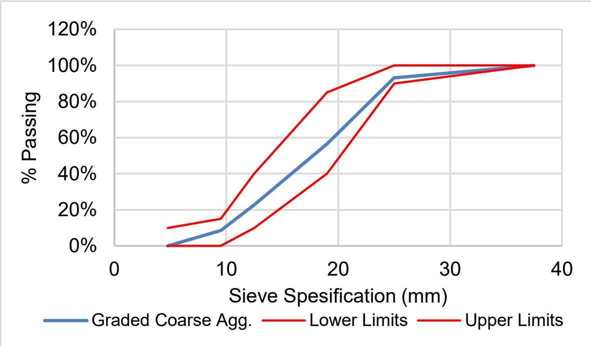

(b)

Figure 1. Sieve Analysis Results: (a). Fine; and (b). Coarse Aggregate.

Table 1. Aggregate Properties

Properties Standard	Fine Aggregate Results	Coarse Aggregate Results	Standard Value
Bulk Density ASTM C – 29	1631 kg/m3	1524 kg/m3	-
Void ASTM C – 29	0.37	0.36	-
SSD Specific Gravity ASTM C – 128	2.63	2.58	Normal aggregate (1.2 - 2.8)
Absorption ASTM C – 128	2.00%	2.97%	Fine agg. max 2.3% Coarse agg. max 3%
Fineness Modulus ASTM C – 136	2.48	-	2.3 - 3.1
Materials Finer than No. 200 Sieve ASTM C – 117	1.7%	0.60%	Fine agg. max 3% Coarse agg. max 1%
Organic Impurities ASTM C – 40	*Standard Plate* No.8	-	-
Resistance to Degradation ASTM C – 131	-	19.22%	max 27%

Source: (American Society of Testing Material ASTM International 2020; ASTM International 2004:40, 2017a:117, 2022a, 2022a:128)

Table 2. Mix Design Proportion

Materials	Weight/ m³	
Cement (C)	639.3	kg/m^3
Fine Aggregates (S)	479.7	kg/m^3
Coarse Aggregates (CA)	1082.0	kg/m^3
Water (W)	179	kg/m^3

Curing Method

Concrete specimens were cured by submersion in water pools with varying salinity levels, based on the target testing age of each batch. Specimens were removed approximately 48 hours prior to testing to allow for surface drying and preparation. The study utilized four curing pools with distinct salinity levels to represent various marine exposure environments. These included: < 0.1%, simulating non-saline (freshwater) conditions; 0.2–0.4%, representing slightly saline or estuarine water; 0.6–0.7%, corresponding to saline lake water; and 3–3.5%, which approximates typical seawater salinity. These categories were based on classifications from the U.S. Geological Survey (USGS). The required salinity in each pool was achieved by proportionally mixing fresh water and seawater sourced from Tanjung Pasir. A handheld refractometer was used to measure salinity in parts per thousand (‰), with adjustments made every 2–3 days to maintain target concentrations.

Two curing methods were employed in this study. The first, called Method A of Curing, involved full-time immersion, where specimens were continuously submerged in the designated curing pool for the entire curing duration (Figure 2). The second method, called Method B of Curing, simulated tidal exposure conditions by transferring specimens between two storage containers every 24 hours, alternating between wet and dry conditions, to replicate tidal fluctuations typically experienced in marine environments (Figure 3).

Testing Methods

This study employed both non-destructive and destructive testing methods to evaluate the mechanical and permeability behavior of concrete specimens.

Non-destructive testing was carried out using the Ultrasonic Pulse Velocity (UPV) method, following ASTM C597 (ASTM International 2022b) and ACI 228 (ACI American Concrete Institute Committee 214 2003) guidelines. UPV testing was performed using the Pundit Lab+ device, which emits 54 kHz electromagnetic pulses. The transducers were positioned on opposite ends of the cylindrical specimens (top and bottom), with an emulsifying gel applied to ensure good acoustic coupling and minimize signal distortion. Prior to testing, the device was calibrated to account for zero-time error. The pulse transit time and wave velocity were recorded and averaged over five trials to ensure measurement reliability. Faster wave propagation is typically associated with denser and more homogeneous concrete, indicating better internal quality (Figure 4).

Compressive strength tests were conducted on cylindrical specimens with a diameter of 150 mm and a height of 300 mm, in accordance with ASTM C39 (ASTM International 2021). Testing ages were set at 7, 28, 42, 56, and 90 days. Each specimen was loaded axially at a constant rate until failure, and the maximum load was recorded (Figure 5).

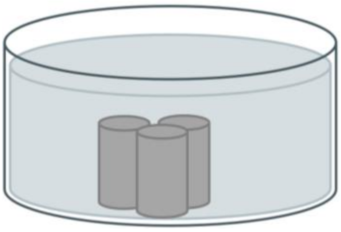

Figure 2. Immersion method A.

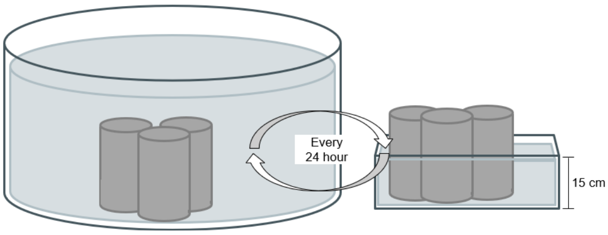

Figure 3. Immersion method B.

Figure 4. Direct method – Ultrasonic Pulse Velocity (UPV) measurement.

Figure 5. Concrete Compressive Test in Laboratory.

Splitting tensile strength tests were performed in accordance with ASTM C496 (ASTM International 2017b) on the same specimen dimensions. Testing was conducted at 28 and 42 days. A compressive load was applied along the longitudinal axis of the cylinder, inducing tensile stress perpendicular to the loading plane. The load was applied gradually without shock until failure occurred. Though tensile strength generally ranges between 9% and 15% of compressive strength, it plays a critical role in resisting crack formation due to shrinkage and thermal effects.

Permeability testing was performed based on the German standard DIN 1048 at 28 and 56 days (ANSI 1991). Water pressure was applied to one face of a cube specimen for a specified period. Afterward, the specimen was split perpendicular to the pressure face to visually inspect and measure the depth of water penetration, which indicates the material's resistance to fluid ingress.

The selection of testing ages—7, 28, 42, 56, and 90 days—was designed to capture both early-age and long-term performance of PCC concrete under varying salinity levels. The 7-day age reflects early strength development, which is critical for construction scheduling and formwork removal decisions. Testing at 28 days corresponds to the standard benchmark age for evaluating concrete strength in structural applications. Additional testing at 42, 56, and 90 days was included to assess the longer-term effects of curing and salinity exposure on mechanical strength and durability-related properties. These extended ages provide insight into the material's performance evolution over time and are particularly relevant for understanding durability in marine or coastal environments where long-term degradation is a concern.

The selected tests and curing conditions were designed to evaluate the time-dependent effects of salinity on strength development, internal quality, and permeability, thereby addressing both structural performance and potential durability concerns.

RESULTS AND DISCUSSION

Compressive Test

Figure 6 presents boxplots illustrating the development of compressive strength in concrete specimens subjected to different salinity levels and curing durations. In general, compressive strength increased with curing time across all salinity conditions, although deviations from the trend were observed.

Specimens from Pool I (<0.1% salinity) exhibited a substantial strength gain up to 28 days, followed by stabilization through 90 days. Pools II and III (0.2–0.4% and 0.6–0.7% salinity, respectively) showed rapid strength development by 7 days, with only marginal increases thereafter. In contrast, Pool IV (3–3.5% salinity) specimens demonstrated a slower early-age strength gain, and a notable decline in strength after 28 days, suggesting possible long-term degradation effects due to higher salinity. Across all conditions, the target compressive strength of 41.4 MPa was not consistently achieved beyond 28 days.

The comparison of curing methods revealed minor differences at 28 and 56 days. However, Curing Method B (simulated tidal exposure) generally resulted in higher strength values compared to Curing Method A (full immersion), particularly in saline environments, as shown in Figure 6. This could be attributed to intermittent drying periods promoting better internal hydration conditions and microstructure refinement.

Several factors may have influenced these outcomes. Fluctuations in water salinity, although corrected regularly, may have temporarily disrupted the hydration process, particularly during the early stages of curing. Variations in the loading rate of the compression testing machine may also have affected results, as higher loading rates are known to yield artificially elevated strength readings due to the brittle nature of concrete. Additionally, differences in casting times, necessitated by mixer capacity constraints, could have introduced inconsistencies among specimens, further contributing to variability in compressive strength outcomes.

Stress–Strain Behavior and Fracture Pattern of 28-Day Specimens

Figure 7 presents the stress–strain relationships for concrete specimens tested at 28 days of age. Under ideal conditions, concrete in compression typically fails at a strain of approximately 0.003. However, in this study, the observed failure strain values varied across the different curing environments. Notably, specimens from Pool II (0.2–0.4% salinity) and Pool III (0.6–0.7% salinity) experienced failure at strain values below the expected threshold (ε_{cu} < 0.003), suggesting a reduced deformation capacity. This premature failure strain may reflect a stiffer but more brittle behavior, possibly due to the influence of salt ions on microcrack propagation and matrix development during early curing.

Table 3 summarizes the observed fracture patterns of specimens tested at 28 days under axial compression. Most specimens exhibited typical vertical or slightly inclined cracks indicative of compressive failure. However, notable variations in crack width, orientation, and fragmentation were observed between salinity conditions.

Table 3. Fracture Patterns of PCC Concrete Sample at 28 Days

Sample	Curing Pool	Crack Pattern (ASTM C39)	Notable Features
A28	Pool I	Type 2	Vertical-diagonal cracks; cone-shaped fracture
A28	Pool II	Type 2	Vertical-diagonal cracks; cone-shaped fracture
A28	Pool III	Type 3	Vertical cracking: upper portion dominated
A28	Pool IV	Type 2	Vertical + diagonal cracks; cone-shaped fracture

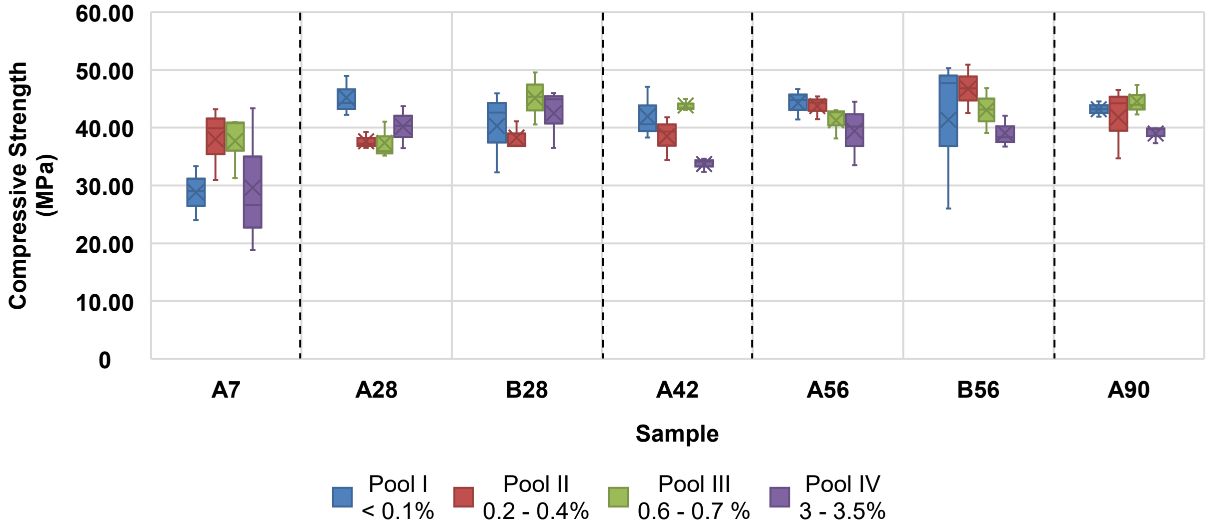

Figure 6. Concrete Compressive Test Results

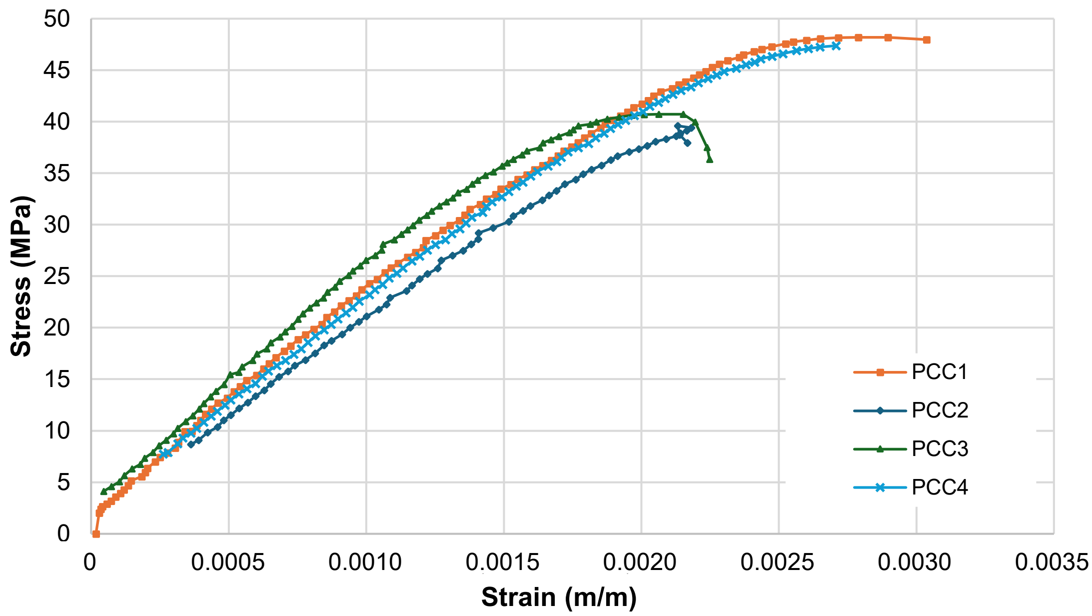

Figure 7. PCC Concrete: Stress-strain relationship

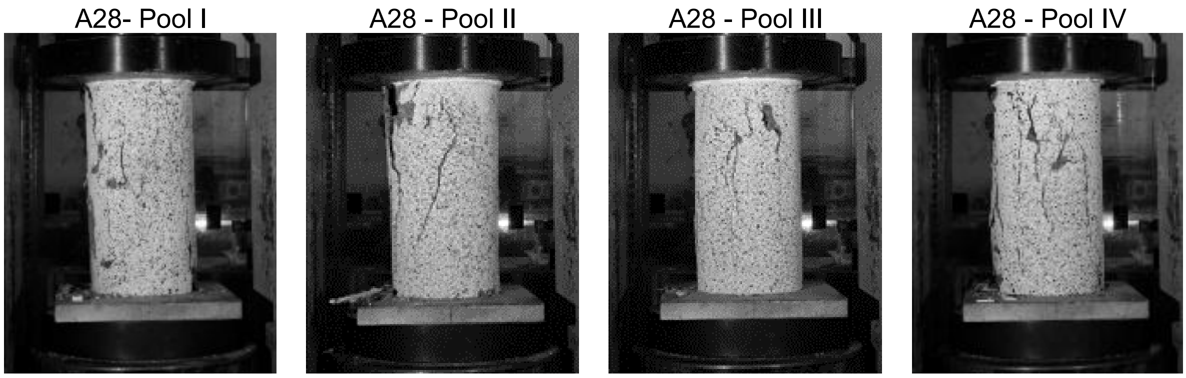

Figure 8. PCC Concrete Fracture Patterns at 28 Days

Specimens cured in low-salinity environments (Pools I and II) tended to show more uniform and well-contained cracking, with vertical splits initiating from the top or bottom edges and propagating along the loading axis. These patterns suggest stable failure with good internal cohesion and relatively ductile behavior.

By contrast, specimens from higher salinity pools (Pools III and IV) exhibited more irregular and fragmented fracture patterns. Cracks often initiated prematurely at mid-height, with wider openings and multiple secondary branches. In some cases, surface spalling and diagonal cracking were also observed, indicating a more brittle failure mode and reduced post-cracking resistance. These behaviors are likely associated with microstructural degradation caused by saline curing environments, such as disrupted cement hydration or weakened interfacial transition zones.

Overall, the variation in crack patterns across salinity levels reflects the influence of curing environment on concrete integrity and fracture characteristics, even when compressive strength values appear comparable.

Compressive Strength and UPV

Figure 9 illustrates the relationship between Ultrasonic Pulse Velocity (UPV) and compressive strength of concrete specimens across various curing durations. As expected, a general trend of increasing UPV with higher compressive strength is observed, particularly in older specimens. This reflects the typical correlation where denser and more homogeneously compacted concrete allows faster wave transmission, indicative of improved internal quality and lower porosity.x

However, the relatively low coefficient of determination (R^2 = 0.247) from the linear regression analysis suggests that the relationship is not strongly linear. This is likely due to multiple interacting factors that affect wave velocity independently of compressive strength, such as microcracking, aggregate distribution, and surface moisture at the time of testing. Furthermore, early-age concrete may show variability in UPV readings due to incomplete hydration and pore structure development, which do not always correlate directly with strength gain.

Despite the weak linear correlation, UPV remains a valuable qualitative indicator of internal concrete condition. When used in conjunction with destructive tests, it can provide supplementary insights into concrete uniformity, potential defects, and the effects of salinity on microstructural integrity.

Splitting Tensile Strength

Figure 10 presents the boxplots of splitting tensile strength results for concrete specimens subjected to different salinity levels and curing durations. In general, tensile strength increased up to 56 days, followed by a decline at 90 days across all pools. This trend suggests strength development continued through mid-term curing, but was negatively affected by prolonged exposure, potentially due to microcracking or delayed degradation in saline conditions.

Among the curing pools, Pool IV (3–3.5% salinity) consistently exhibited the lowest tensile strength values, indicating the detrimental effects of high salinity on crack resistance. Interestingly, Pool II (0.2–0.4% salinity) showed higher tensile strength than Pool I (freshwater), possibly due to a densifying effect of mild salinity on early hydration and matrix compaction. However, this effect did not persist at higher salinity levels, suggesting a narrow range of potentially beneficial salt concentration.

Relationship between Splitting Tensile and Compressive Strength

A strong empirical relationship typically exists between concrete's compressive and splitting tensile strengths, often represented by a proportional constant k, which varies depending on mix composition, strength class, and curing conditions (Russell et al. 1998). In this study, the k values ranged from 0.36 to 0.44, with an overall average of 0.40 across all salinity conditions.

This suggests that, on average, the tensile strength corresponded to approximately 6% of the compressive strength, which is slightly below typical values reported for high-strength concrete (often in the range of 8–10%). The relatively low tensile-to-compressive strength ratio may indicate increased susceptibility to tensile cracking, especially under flexural or thermal stresses. From a structural design perspective, this emphasizes the importance of adequate reinforcement in tension zones when using PCC concrete in saline environments.

Splitting Tensile Strength and Ultrasonic Pulse Velocity (UPV)

Figure 11 illustrates the relationship between Ultrasonic Pulse Velocity (UPV) and the splitting tensile strength of concrete specimens. While a general trend can be observed—where higher UPV values correspond to higher tensile strength, the correlation is weak. The coefficient of determination for the linear regression is $R^2 = 0.072$, indicating that UPV is not a strong predictor of tensile strength under the conditions tested.

The weak correlation may be attributed to the fact that UPV is more sensitive to overall internal density and homogeneity, while splitting tensile strength is influenced more directly by localized flaws, interfacial transition zones, and aggregate-paste bonding quality. Additionally, microcracks formed during curing—especially in saline environments—may not significantly affect wave velocity but could still act as initiation points for tensile failure.

Despite the weak quantitative relationship, UPV remains useful as a qualitative indicator of concrete integrity and can help screen for internal inconsistencies. However, it should not be relied upon as a standalone predictor of tensile strength in concretes exposed to variable curing conditions.

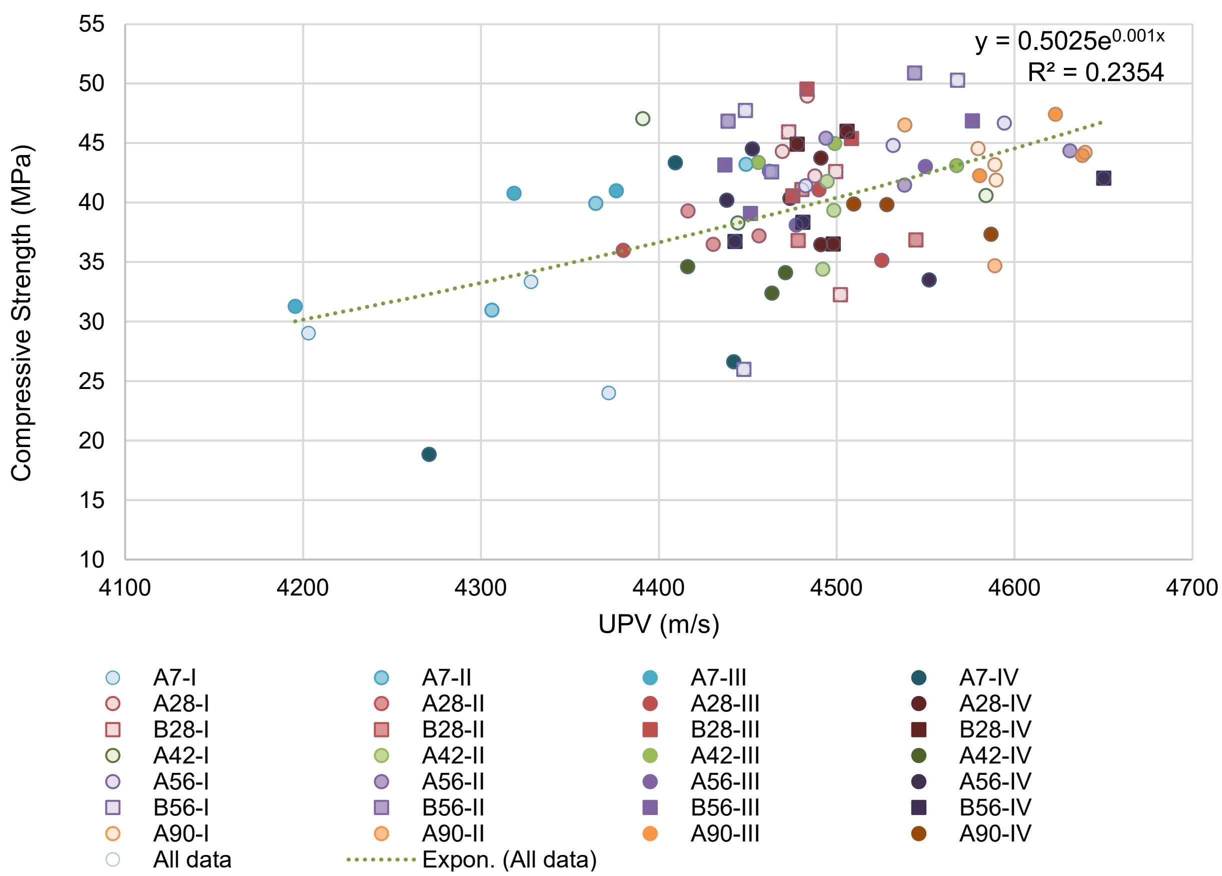

Figure 9. Relationship Between Compressive Strength and UPV

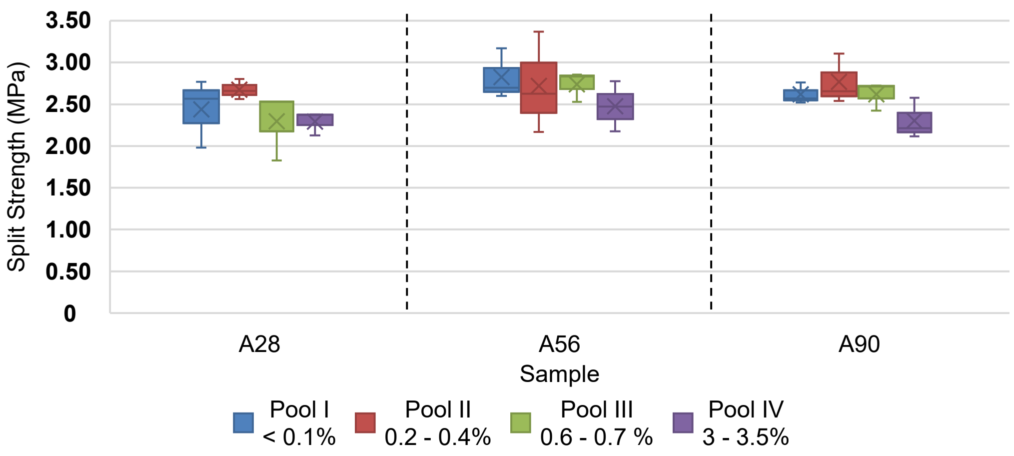

Figure 10. Split Tensile Strength Test Results

Table 4. Relationship between Split Tensile and Compressive Strength

Sample	Tensile Strength (MPa)	Average Splitting Tensile Strength (MPa)	Compressive Strength (MPa)	Average Compressive Strength (MPa)	Tensile/Compressive Strength Ratio	k
A28-I	2.77	2.44	44.30	45.16	5%	0.36
	2.57		42.24			
	1.98		48.96			
A28-II	2.56	2.67	37.21	37.66	7%	0.44
	2.66		36.50			
	2.80		39.29			
A28-III	2.53	2.30	35.14	37.40	6%	0.38
	1.83		41.06			
	2.53		35.98			
A28-IV	2.37	2.29	40.35	40.19	6%	0.36
	2.13		43.74			
	2.38		36.48			
A56-I	2.70	2.82	41.42	44.30	6%	0.42

Sample	Tensile Strength (MPa)	Average Splitting Tensile Strength (MPa)	Compressive Strength (MPa)	Average Compressive Strength (MPa)	Tensile/Compressive Strength Ratio	k
	3.17		44.79			
	2.60		46.68			
A56-II	3.37	2.72	45.41	43.74	6%	0.41
	2.62		41.47			
	2.17		44.35			
A56-III	2.83	2.74	42.64	41.26	7%	0.43
	2.85		38.11			
	2.53		43.03			
A56-IV	2.47	2.47	44.50	39.40	6%	0.39
	2.78		40.19			
	2.17		33.51			
A90-I	2.76	2.62	43.19	43.21	6%	0.40
	2.52		44.55			
	2.57		41.89			
A90-II	3.11	2.77	34.68	41.81	7%	0.43
	2.65		44.22			
	2.54		46.53			
A90-III	2.72	2.62	43.96	44.55	6%	0.39
	2.42		42.27			
	2.71		47.41			
A90-IV	2.12	2.30	39.82	39.01	6%	0.37
	2.21		39.88			
	2.58		37.33			

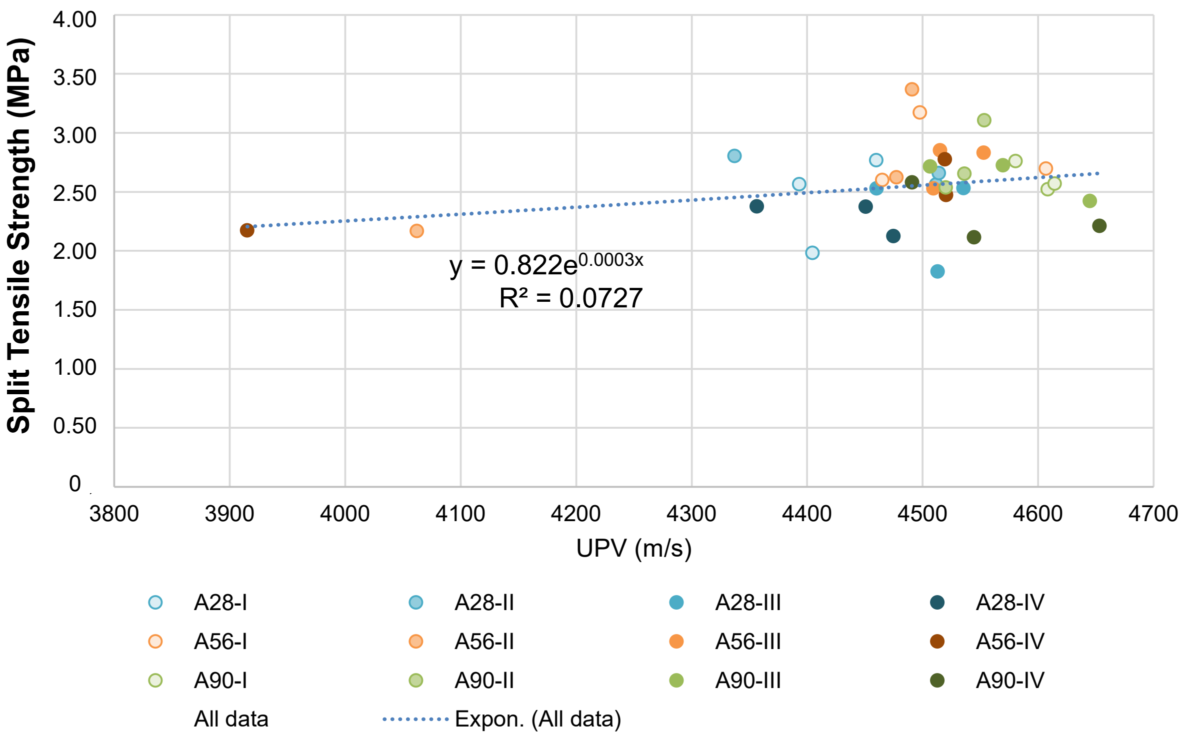

Figure 11. Strong Relationship between Split Tensile and UPV.

Permeability test

Figure 12 presents the results of the concrete permeability tests conducted at 28 and 56 days for specimens cured under varying salinity conditions. Overall, concrete samples exposed to saline environments (Pools II, III, and IV) exhibited lower permeability values compared to the control group (Pool I with <0.1% salinity). Additionally, permeability generally decreased with longer curing durations, consistent with ongoing hydration and pore refinement over time.

These results are somewhat counterintuitive, as exposure to sulfates and salts is typically expected to increase permeability due to microcracking and expansive reactions. One possible explanation is the crystallization of salt within the pore structure, which may have partially blocked capillary channels, thereby reducing water penetration during the test. However, this hypothesis was not supported by UPV measurements. A correlation analysis between permeability and UPV yielded a very low coefficient of determination (R^2 = 0.0053), indicating no meaningful relationship between the two parameters.

This correlation suggests that salt-induced changes to permeability may not be related to improvements in material density or homogeneity, but rather to pore blockage or surface effects not captured by UPV. Further microstructural analysis would be needed to confirm the presence of salt crystallization and its long-term durability implications.

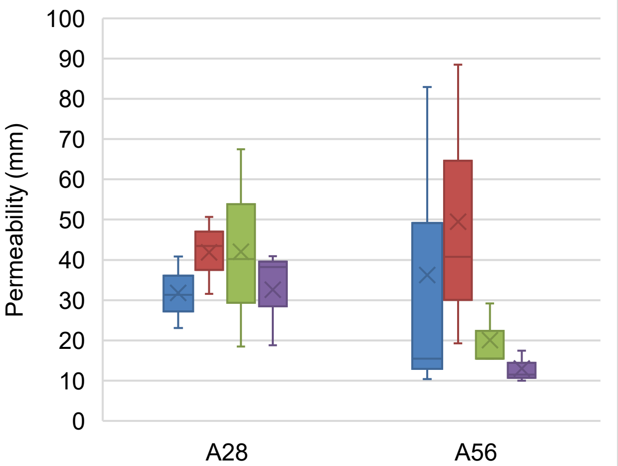

Figure 12. Concrete permeability Test Results

CONCLUSION

This study evaluated the mechanical and durability-related properties of concrete made with Portland Composite Cement (PCC) under varying salinity conditions. The results showed that compressive strength generally increased with longer curing durations, and Ultrasonic Pulse Velocity (UPV) measurements reflected improved internal quality over time. The choice of curing method had a limited influence on strength development, though Curing Method B (simulated tidal exposure) occasionally resulted in slightly higher compressive strength values.

Concrete exposed to high salinity levels exhibited reduced splitting tensile strength and greater susceptibility to cracking, highlighting the need for additional reinforcement when used in aggressive environments. Interestingly, permeability testing revealed improved watertightness in specimens subjected to high salinity, which contradicts typical expectations. This unexpected result may suggest salt crystallization within pore structures, although this hypothesis was not supported by UPV data, which showed no clear indication of increased density or structural compaction. Based on the findings, PCC concrete appears suitable for use in environments with low salinity (<1%), such as areas affected by mild seawater intrusion.
Future research is recommended to develop higher-strength concrete by incorporating performance-enhancing additives in accordance with SNI 03-6468-2000, ensuring mix consistency through single-batch casting, and increasing sample quantities to improve statistical reliability. Control over slump, water-to-cement (w/c) ratio, and curing conditions—such as temperature, evaporation, and contamination—should also be prioritized to minimize variability. To investigate the potential effects of salt crystallization and long-term durability in saline environments, future studies should include microstructural analysis techniques such as Scanning Electron Microscopy (SEM), X-ray Diffraction (XRD), and X-ray Fluorescence (XRF). In addition, exploring other environmentally friendly cement types, such as Portland Pozzolan Cement (SNI 0302:2014) (Nasional 2023a), Portland Slag Cement (SNI 8363:2023) (Nasional 2023c), and Fly Ash-Based Cement (SNI 6468:2023) (Nasional 2023b), is encouraged. Fly ash, as a supplementary cementitious material with pozzolanic properties, has shown promise in improving sulfate resistance and long-term durability, and its integration could further enhance the sustainability and resilience of concrete used in coastal infrastructure.

ACKNOWLEDGEMENT

The authors express their gratitude to PT Semen Indonesia (Persero) Tbk and PT Adhi Mix for providing cement materials, and to PT Pancaran Sewu Sejahtera for providing laboratory space and equipment support.

FUNDING

This study was supported by research funding and material provisions from PT Semen Indonesia (Persero) Tbk.

DATA AVAILABILITY STATEMENT

The data presented in this study are available upon request from the corresponding author.

ACKNOWLEDGMENT

The authors express their gratitude to PT Semen Indonesia (Persero) Tbk and PT Adhi Mix for providing cement materials, and to PT Pancaran Sewu Sejahtera for providing laboratory space and equipment support.

CONFLICTS OF INTEREST

The authors declare no conflict of interest.

REFERENCES

ACI American Concrete Institute Committee 214. (2003). 'ACI 228.1R-03: In-Place Methods to Estimate Concrete Strength'. https://www.concrete.org/store/productdetail.aspx?ItemID=228103&Format=DOWNLOAD&Language=English&Units=US_AND_METRIC.

American Society of Testing Material ASTM International. (2020). 'ASTM C131 / C131M - 20 Standard Test Method for Resistance to Degradation of Small-Size

Coarse Aggregate by Abrasion and Impact in the Los Angeles Machine'.

American Society of Testing Material ASTM International, ASTM. (2008). 'ASTM C33 / C33M - 08 Standard Specification for Concrete Aggregates'.

ANSI, DIN. (1991). 'DIN 1048-5:1991 - Testing Concrete; Testing of Hardened Concrete (Specimens Prepared in Mould) (FOREIGN STANDARD)'.

ASTM International, American Society for Testing and Materials. (2004). 'ASTM C40-04. Standard Test Method for Organic Impurities in Fine Aggregates for Concrete'.

ASTM International, American Society for Testing and Materials. (2017a). 'ASTM C117-17 Standard Test Method for Materials Finer than 75-Mm (No. 200) Sieve in Mineral Aggregates by Washing'.

ASTM International, American Society for Testing and Materials. (2017b). 'ASTM C496/C496M-17 Standard Test Method for Splitting Tensile Strength of Cylindrical Concrete Specimens'.

ASTM International, American Society for Testing and Materials. (2021). 'ASTM C39/C39M-21, Standard Test Method for Compressive Strength of Cylindrical Concrete Specimens'.

ASTM International, American Society for Testing and Materials. (2022a). 'ASTM C128-22 Standard Test Method for Relative Density (Specific Gravity) and Absorption of Fine Aggregate'.

ASTM International, American Society for Testing and Materials. (2022b). 'ASTM C597-22 Standard Test Method for Ultrasonic Pulse Velocity Through Concrete'.

BSN Badan Standarisasi Nasional, BSN Badan Standarisasi Nasional. (2013). 'SNI 15-2049-2004 Semen Portland'. *Jakarta: Badan Standarisasi Nasional*. https://dwikusumadpu.wordpress.com/rak-kode/21376_sni_15-2049-2004-semen-portland/.

Ernawan, Eristra, Jessica Sjah, Nuraziz Handika, Sotya Astutiningsih, and Eric Vincens. (2023). 'Mechanical Properties of Concrete Containing Ferronickel Slag as Fine Aggregate Substitute Using Digital Image Correlation Analysis'. *Buildings* 13(6):1463. doi:10.3390/buildings13061463.

Feiz, Roozbeh, Jonas Ammenberg, Leenard Baas, Mats Eklund, Anton Helgstrand, and Richard Marshall. (2015). 'Improving the CO2 Performance of Cement, Part I: Utilizing Life-Cycle Assessment and Key Performance Indicators to Assess Development within the Cement Industry'. *Journal of Cleaner Production* 98:272–81. doi:10.1016/j.jclepro.2014.01.083.

Gibbs, Michael J., Peter Soyka, and David Conneely. (2001). 'CO2 Emissions from Cement Production: IPCC Guidelines'. *Good Practice Guidance and Uncertainty Management in National Greenhouse Gas Inventories*. https://studylib.net/doc/18357466/co2-emissions-from-cement-production.

Handika, Nuraziz, Balqis Fara Norita, Elly Tjahjono, and Essy Arijoeni. (2021). 'Experimental Studies on the Homogeneity and Compressive Strength Prediction of Recycled Aggregate Concrete (RAC) Using Ultrasonic Pulse Velocity (UPV)'. doi:https://doi.org/10.32783/csid-jid.v3i2.111.

Handika, Nuraziz, M. Rafky, S. Danifaro, Elly Tjahjono, and Essy Arijoeni. (2021). 'Homogeneity of Papercrete with 10% Waste Paper Substitution Using Ultrasonic Pulse Velocity (UPV)'. *AIP Conference Proceedings* 2376(1):040005. doi:10.1063/5.0063943.

IRICEN, Pune. (2014). 'INDIAN RAILWAYS INSTITUTE OF CIVIL ENGINEERING'.

Mangasi, Yudhistira J. U., Nadhifah K. Kirana, Jessica Sjah, Nuraziz Handika, and Eric Vincens. (2024). 'Correlation of Rebound Hammer and Ultrasonic Pulse Velocity Methods for Instant and Additive-Enhanced Concrete'. *Structural Monitoring and Maintenance* 11(1):41–55. doi:https://doi.org/10.12989/smm.2024.11.1.041.

Mehta, P. K. (1983). 'Mechanism of Sulfate Attack on Portland Cement Concrete — Another Look'. *Cement and Concrete Research* 13(3):401–6. doi:10.1016/0008-8846(83)90040-6.

Nasional, BSN Badan Standarisasi. (2022). 'SNI 7064 2022 Semen Portland Komposit (PCC, Portland Cement Composite)'.

Nasional, BSN Badan Standarisasi. (2023a). 'SNI 0302:2014 Semen Portland Pozolan'.

Nasional, BSN Badan Standarisasi. (2023b). 'SNI 6468:2023 Panduan Untuk Pemilihan Proporsi Beton Berkekuatan Tinggi Menggunakan Semen Portland Dan Material Sementisius Lainnya (ACI 211.4R-08, IDT)'.

Nasional, BSN Badan Standarisasi. (2023c). 'SNI 8363:2023 Semen Portland Slag (ASTM C595/C595M-21, MOD)'.

Neville, A. M. 2011. *Properties of Concrete: Properties of Concrete, 5th Edition[Book]*. 5th Edition. Pearson.

Qasim, Ola Adel, Baydaa Hssain Maula, Hayder Hussein Moula, and Salim H. Jassam. (2020). 'Effect of Salinity on Concrete Properties'. *IOP Conference Series: Materials Science and Engineering* 745(1):012171. doi:10.1088/1757-899X/745/1/012171.

Russell, Henry G., Chairman, Arthur R. Anderson, Jack O. Banning, Irwin G. Cantor, Ramon L. Carrasquillo, James T. E. Cook, Gregory Clayton Frantz, Weston T. Hester, David Anderson, Claude Bédard, Roger W. Black, Judith A. Castello, Kingsley D. Drake, Thomas G. Guennewig, Anthony N. Kojundic, Brian R. Mastin, William C. Moore, Arthur H. Nilson, William F. Perenchio, Francis J. Principe, N. L. Howard, Mark D. Luther, Heshem Marzouk, Jaime Moreno, Clifford R. Ohwiler, Secretary, Kenneth L. Saucier, Surendra P. Shah, J. Craig Williams, and John T. Wolsiefer. (1998). 'ACI 363 R-98 (Reapproved 1997) State-Ofthe-Art Report on High-Strength Concrete Reported by ACI Committee 363'. https://www.semanticscholar.org/paper/ACI-363-R-92-(-Reapproved-1997-)-State-ofthe-Art-on-Russell-Chairman./2bf39412b2393af4ed05c913922a5c0980ab2f50.

SIG, PT Semen Indonesia (Persero). (2023). *Embracing Challenges to Advance in A Sustainable Future*. PT Semen Indonesia (Persero).

Tian, Bing, and Menashi D. Cohen. (2000). 'Does Gypsum Formation during Sulfate Attack on Concrete Lead to Expansion?' *Cement and Concrete Research* 30(1):117–23. doi:10.1016/S0008-8846(99)00211-2.

United Nations Environment Programme, UNEP, and GlobalABC Global Alliance for Buildings and Construction. (2024). 'Global Status Report for Buildings and Construction: Beyond Foundations: Mainstreaming Sustainable Solutions to Cut Emissions from the Buildings Sector'. (CLI/2621/NA). doi:https://doi.org/10.59117/20.500.11822/45095.